FEBS Letters 586 (2012) 740–746

FEBS Letters

journal homepage: www.FEBSLetters.org

# MIG-13 controls anteroposterior cell migration by interacting with UNC-71/ADM-1 and SRC-1 in *Caenorhabditis elegans*

Hitomi Masuda [a], Kuniaki Nakamura [b,2], Nozomu Takata [a,1], Bunsho Itoh [a], Takashi Hirose [c], Hiroki Moribe [b,3], Eisuke Mekada [b], Masato Okada [a,*]

[a] Department of Oncogene Research, Research Institute for Microbial Diseases, Osaka University, 3-1 Yamadaoka, Suita Osaka 565-0871, Japan
[b] Department of Cell Biology, Research Institute for Microbial Diseases, Osaka University, 3-1 Yamadaoka, Suita Osaka 565-0871, Japan
[c] Howard Hughes Medical Institute and Department of Biology, Massachusetts Institute of Technology, Cambridge, MA 02139, USA

ARTICLE INFO

*Article history:*
Received 19 December 2011
Revised 16 January 2012
Accepted 16 January 2012
Available online 27 January 2012

Edited by Ned Mantei

*Keywords:*
Neural development
Q neuroblast
ADAM
Src
MIG-13

ABSTRACT

**The transmembrane protein MIG-13 is a key regulator required for anterior migration of neural cells in *Caenorhabditis elegans*, but the signaling mechanisms involved remain unknown. Here, we isolated a suppressor mutation in the *unc-71/adm-1* gene, which rescued the AVM neuron migration defect in *mig-13* mutants. Genetic analyses revealed that UNC-71 at least partly acts downstream of MIG-13 and has an inhibitory effect on the anterior cell migration. The *unc-71* mutation also rescued the anterior migration defect of AVM neuron in *src-1* mutants. These findings suggest that MIG-13 controls anteroposterior cell migration by interacting with UNC-71 and SRC-1 in *C. elegans*.**


## 1. Introduction

Cell migration is crucial for normal development of multicellular organisms and its underlying mechanism is functionally conserved during evolution [1,2]. Aberrant cell migration leads to severe embryonic malformations and defects in tissue organization and homeostasis that cause various disorders [3]. The nematode *Caenorhabditis elegans* is an excellent model for studying how cell migration is regulated during development [4,5]. A number of proteins related to cell migration in *C. elegans* have been identified. For example, the netrin/UNC-6, slit/SLT-1 and TGF-β/UNC-129 signaling pathways play crucial roles in regulating the global guidance of cells and axons along the dorsoventral axis [6–8]. As for anteroposterior (A/P) migration, the transcription factor HAM-2 is required to direct migration of HSN motor neurons by acting downstream of a Homeobox gene, *egl-5* [9]. In the sex myoblast (SM), an FGF-like ligand EGL-17 [10] and a receptor belonging to the FGF receptor subfamily EGL-15 [11] are crucial for proper positioning of SM. Nonetheless, signaling mechanisms that control global guidance along the A/P axis still remain obscure.

*C. elegans* Q neuroblasts, QR and QL are born at similar anterior-posterior positions on the right and left side of the body, but they migrate in opposite directions; QL and its descendants migrate toward the posterior, whereas QR and its descendants migrate toward the anterior [12]. These migrations are regulated cell autonomously by two homeobox genes, *mab-5* and *lin-39*. Expression of *mab-5* is induced specifically in the QL lineage by Wnt/EGL-20 signaling and promotes the posterior migration of QL and its descendants [13–15]. *mab-5* is not expressed in the QR lineage; instead, *lin-39* promotes anterior migration of the QR lineage [16]. However, extracellular signalings acting in these migrations need to be addressed.

The *mig-13* gene is known to play a key role in promoting anterior cell migration along the A/P axis. *mig-13* encodes a novel transmembrane protein with an LDL receptor repeat and a CUB domain, and is expressed in the anterior body region. *mig-13* acts non-cell autonomously as a component of the global guidance system along the A/P axis. [17]. *mig-13* also acts in parallel to *lin-39*, and interacts generally with the Hox co-factor orthologs, *ceh-20* and *unc-62* [17,18]. However, the molecular mechanisms underlying MIG-13 function remain unknown.

* Corresponding author. Fax: +81 6 6879 8298.
*E-mail address:* okadam@biken.osaka-u.ac.jp (M. Okada).
[1] Present address: Neurogenesis and Organogenesis Group, RIKEN Center for Developmental Biology, Kobe 650-0047, Japan.
[2] Present address: Takeda Pharmaceutical Company Limited, 2-17-85 Jusohon-machi, Yodogawa-ku, Osaka 532-8686, Japan.
[3] Present address: Department of Biology, School of Medicine, Kurume University, 67 Asahi-machi, Kurume-shi, Fukuoka-ken 830-0011, Japan.

0014-5793/$36.00 
doi:10.1016/j.febslet.2012.01.031

To address the mechanisms of the MIG-13 pathway, we screened for mutations that suppress the defects in *mig-13* mutants. We isolated a suppressor mutant with a loss-of-function mutation in the *unc-71/adm-1* gene, which encodes a disintegrin and metalloprotease (ADAM) protein [19]. We found that UNC-71 at least partly acts downstream of MIG-13 through being down-regulated in its inhibitory effect on the anterior cell migration. Moreover, UNC-71 acts in the same pathway as SRC-1, a signaling tyrosine kinase required for controlling cell migration. These findings suggest that MIG-13 controls A/P cell migration via a novel signaling interaction with UNC-71/ADM-1 and SRC-1 in *C. elegans*.

## 2. Materials and methods

### 2.1. Isolation of mig-13 suppressor mutants

Animals homozygous for *mig-13(mu225)* were mutagenized with 50 mM ethylmethane sulfonate (EMS) [5]. F2 progeny were screened for mutations that rescue the aberrant position of AVM neuron (QR.paa) in *mig-13* mutants. The *mec-7-gfp* transcriptional fusion, *muIs32*, is strongly expressed in the mechanosensory neurons including AVM neuron [20], and was used to visualize AVM neuron position by fluorescence stereomicroscopy.

### 2.2. Cloning and transformation rescue of unc-71

Genomic DNA from N2 animals was isolated following standard procedures [21]. The *unc-71* genomic region was amplified using a long range PCR kit (Roche). The DNA mixture for *unc-71* rescue consisted of three overlapping PCR products covering the entire *unc-71* coding region, as well as 5 kb 5′-flanking and 2 kb 3′-flanking sequences. To rescue the *ov10* phenotype, the DNA mixture (50 ng/μl) was injected with a *Plin-44::gfp* injection marker (50 ng/μl) into the *sup-1(ov10); mig-13(mu225); muIs32[Pmec-7::gfp]* animals in the young adult stage. Transgenic lines were obtained using standard protocol [22].

### 2.3. Phenotypic analysis

AVM (QR.paa), PVM (QL.paa) and BDU neurons were visualized using a *mec-7-gfp* transcriptional fusion, *muIs32*, which is expressed in mechanosensory neurons including AVM and PVM, FLP, PVD, and BDU neurons. Their positions were scored relative to V-cell daughters, which were used as stationary landmarks at the end of the L1 stage [20]. QR lineage migration in living animals was directly observed on a 5% agar pad in M9 buffer using Nomarski optics.

### 2.4. RNA interference

RNAi was performed in the background of *rrf-3(pk1426)*, which are more sensitive to RNAi than wild-type animals [23]. The *unc-71* dsRNA sequence was designed as previously described [24], and was synthesized from pCZ418 (gift of Dr. Y. Jin) [19], as previously described [25]. The dsRNA (50 ng/μl) was injected with a *Plin-44::gfp* injection marker (50 ng/μl) into *mig-13(mu225); rrf-3(pk1426); muIs32[Pmec-7::gfp]* and *rrf-3(pk1426); muIs32 [Pmec-7::gfp]* animals in L4. Injected animals were put onto plates and their late L1 progeny were analyzed for AVM neuron position.

### 2.5. Ectopic expression of mig-13

Ectopic expression of *mig-13* was carried out as described previously [18]. The *mig-13* cDNA was amplified by PCR, and the *mig-13-gfp* translational fusion was constructed by inserting the GFP coding region of pPD95.75 into the XhoI site in the last exon of the *mig-13* cDNA. The resulting construct was inserted into the H20 promoter vector. The *PH20::mig-13::gfp* (50 ng/μl) was injected with a *Plin-44::gfp* injection marker (50 ng/μl) into the *muIs32* young adults. We first made the extrachromosomal array in wild-type background, and then crossed these animals into *mig-13(mu225)*, *lin-39(n1760)*, and *src-1(cj293)*. We analyzed a homozygous *src-1(cj293)* mutant produced from the balanced heterozygote *src-1(cj293)/+*, as the *src-1(cj293)* mutant showed a maternal embryonic lethal phenotype [26].

## 3. Results

### 3.1. Isolation of a mutant that suppresses the migration defect in mig-13 mutants

In wild-type animals, QR and its descendants migrate anteriorly along the A/P axis, and the AVM neuron (QR.paa) ends up between the V1.p and V2.a cells (Fig. 1). In *mig-13(mu225)* mutants, QR migrates anteriorly a short distance as in wild-type animals, but its descendants, particularly QR.a, QR.p, and QR.pa, end their migration prematurely. As a result, QR descendants, including AVM neurons, end up being located in a more posterior position that in wild-type animals (Fig. 1) [13,17]. To identify genes involved in the MIG-13 pathway, we screened mutants that rescue these migration defects of QR descendants in *mig-13(mu225)* mutants. We mutagenized *mig-13(mu225); muIs32[Pmec-7::gfp]* animals and screened mutants with rescued AVM neuron position, using the *mec-7-gfp* transcriptional fusion *muIs32* as a marker of mechanosensory neurons, including the AVM neuron [20]. From more than 10 000 mutagenized haploid genomes screened, we isolated a suppressor mutant, *sup-1 (ov10)*, which partially rescues the AVM neuron position defect (Fig. 1A).

In *sup-1(ov10); mig-13(mu225)* double-mutants, AVM neurons were located in a more anterior position than in *mig-13(mu225)* mutants (Fig. 1C). Live observation revealed that the *ov10* mutation rescued the *mig-13(mu225)* AVM neuron position defect by extending the migration distance of QR descendants (Fig. 1B). In the double-mutants, however, the majority of QR descendants stopped migration at around the position of the V2.a cell (Fig. 1C). Also, the migration defects of BDU neurons in the anterior body region of *mig-13* mutants were not significantly rescued by the *ov10* mutation (Fig. 1D). These observations indicate that the *ov10* mutation can rescue the early phase of the anterior migration of these cells up to the mid-body region, and suggest that *ov10* is at least partly linked to the MIG-13 pathway.

### 3.2. Mapping and cloning of ov10

We next identified the gene responsible for the *ov10* mutation. SNP mapping analysis revealed that the *ov10* mutation is located to the right of the SNP allele pKP3114, which is at +17.99 on LGIII [27,28]. We narrowed down the location of the *ov10* mutation to between +17.99 and +19.53 by deficiency mapping of *ctDf3* (Fig. S1A) [29]. The corresponding genomic region from 12497894 to 12951561 bp on LGIII was then subjected to next-generation sequencing. We found a single C-to-T substitution in the *unc-71/adm-1* coding region (Fig. S1A), which changes a glutamine codon to a stop codon in the middle of disintegrin domain, suggesting that *ov10* may express a truncated form of UNC-71 (Fig. S1B).

### 3.3. ov10 is unc-71/adm-1 mutant

To confirm that the *unc-71* mutation underlies the suppressor phenotype in *ov10* animals, we examined whether the *unc-71* gene

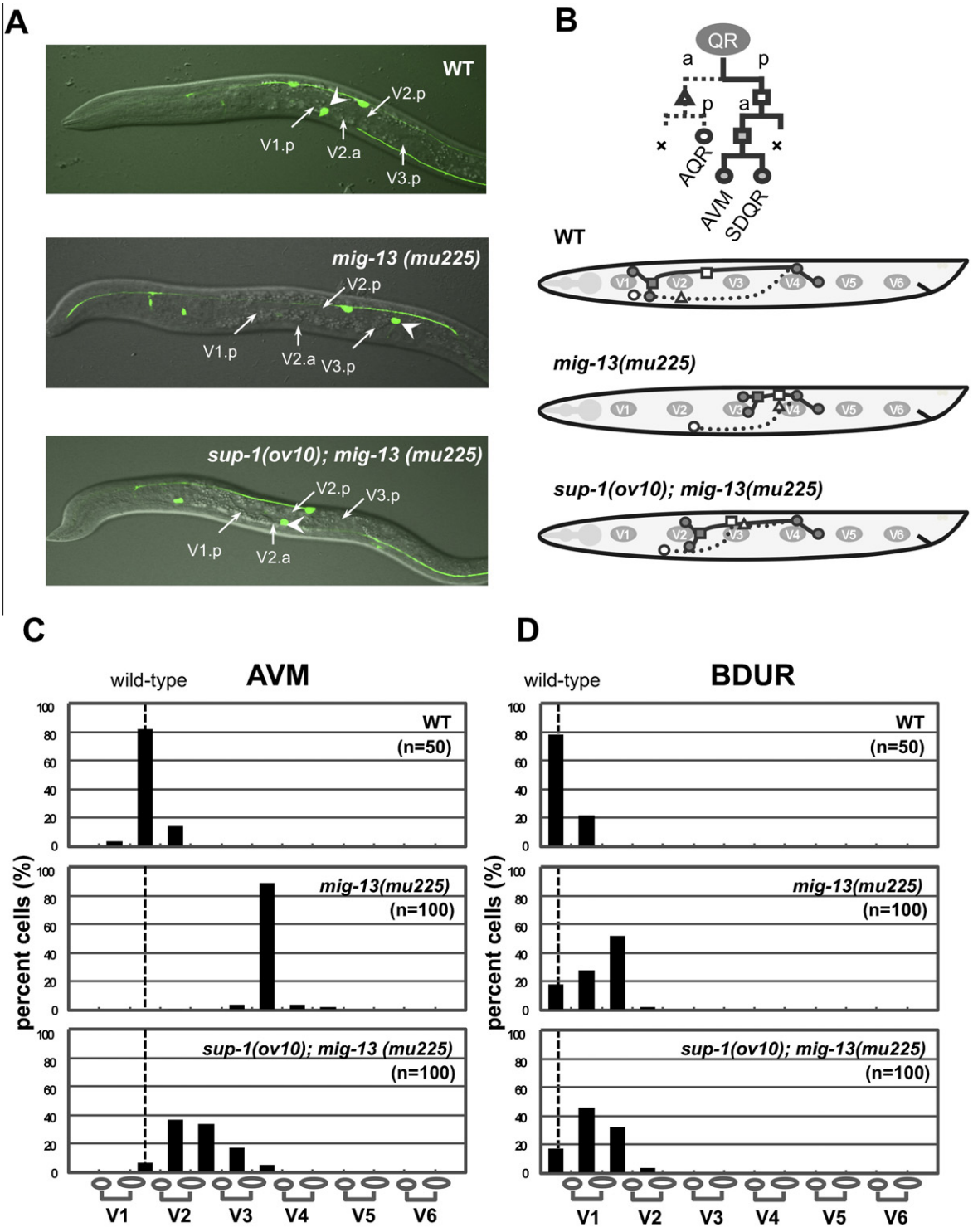


**Fig. 1.** *ov10* suppresses the cell migration defect of *mig-13(mu225)* mutants. (A) The AVM neuron positioning in L1 late animals. All animals carried the *muIs32[Pmec-7::gfp]* transgene to visualize the AVM neuron and other mechanosensory neurons. GFP and DIC images were merged. Arrows indicate nuclei of V-cells. Arrowheads indicate AVM neurons. (B) The migration of QR and its descendants in the indicated strains. The upper panel shows a lineage diagram. The solid line indicates migration of QR.p and its descendants. The dashed line indicates migration of the QR.a descendant. Triangle and square symbols represent cell divisions. (C) Final AVM (QR.paa) neuron positions in the indicated strains are scored relative to V-cell daughters, which are used as stationary landmarks. The dashed line indicates the final position of the AVM neuron in wild-type animals. The number of cells scored is indicated in each graph. (D) Final BDUR positions in the indicated stains are scored relative to V-cell daughters, which are used as stationary landmarks. The dashed line indicates the final position of BDUR in wild-type animals. The numbers scored are indicated in each graph.

is able to rescue the *ov10* phenotype by germline transformation. The *ov10* phenotype was rescued in the transgenic animals, with the AVM neuron position similar to that in *mig-13(mu225)* mutants (Fig. 2A). Furthermore, we crossed *mig-13(mu225)* mutants to other *unc-71* alleles, *ju156* and *e541* [19]. *ju156* has a premature stop before the metalloprotease domain due to a 170 bp deletion in Exon2 and is thought to a null mutation. *e541* is a missense mutation in the cysteine-rich domain. Both alleles could rescue

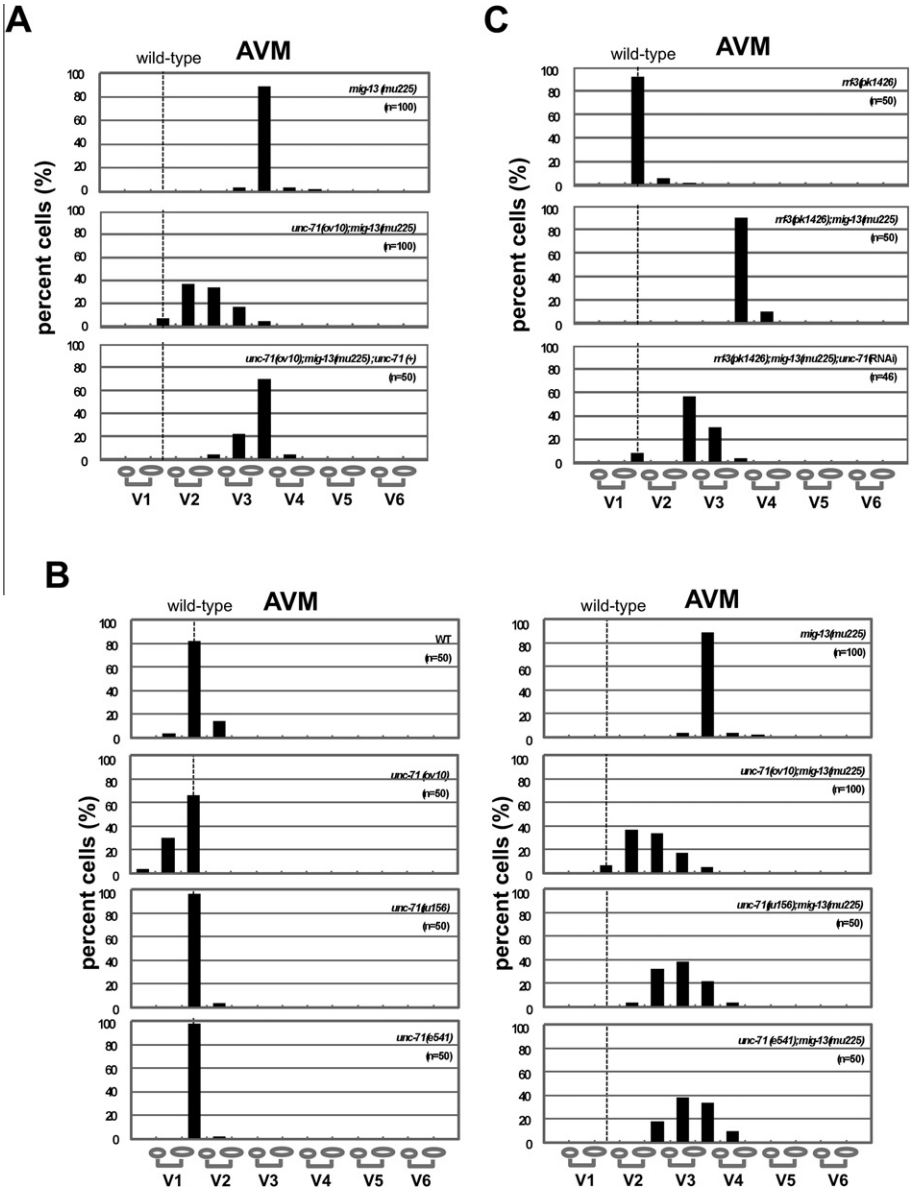


**Fig. 2.** *ov10* is *unc-71* mutant. (A) Final AVM neuron positions in the indicated strains are scored. *unc-71* DNA was injected into *sup-1(ov10)*; *mig-13(mu225)*; *muIs32[Pmec-7::gfp]* animals. The AVM neuron position in *unc-71* transgenic animals reverted to that of *mig-13* mutants (bottom panel). (B) Final AVM neuron positions for three different *unc-71* alleles (*ov10*, *ju156* and *e541*) are scored. The results for *unc-71* single mutants (left panels) and *unc-71*; *mig-13* double mutants (right panels) are shown. The AVM neuron position defect in *mig-13* mutants is suppressed by these *unc-71* alleles. (C) Effects of *unc-71* RNAi on the *mig-13* phenotype are scored.

the AVM neuron position defect in *mig-13* mutants, although single mutants of these alleles exhibited no defects (Fig. 2B). These results indicate that the *unc-71* mutation can serve as a suppressor of the *mig-13* mutation.

We also found that the *ov10* mutation more strongly rescued the *mig-13* phenotype than did the *e541* mutation (Fig. 2B), suggesting that both of the disintegrin domain and the cysteine-rich domain are required for the activity that disrupts the migration of QR descendants. However, the *ov10* phenotype was also stronger than that of *ju156*. In some of the *unc-71(ov10)* animals, the AVM neuron position was shifted more anteriorly than its normal position (Fig. 2B). These observations suggest that the *unc-71(ov10)* mutation, but not the *unc-71(e541)* or *unc-71(ju156)* mutation, may have another epistatic effect by expressing the truncated form of UNC-71.

To determine whether these phenotypes indeed resulted from the reduced *unc-71* activity, we carried out *unc-71* RNAi using the *rrf-3(pk1426)* strain, in which neuronal RNAi is enhanced [23]. In the *rrf-3(pk1426)* background, wild-type and *mig-13(mu225)* exhibited the same phenotype as in the N2 background (Fig. 2C). *unc-71* RNAi suppressed the migration defect of AVM neurons in *mig-13* mutants, as seen in *unc-71(ov10); mig-13(mu225)* animals (Fig. 2C); however it had no effect on the *rrf-3(pk1426)* strain (data not shown). These results indicate that the suppressor effect of *ov10* on the defect in *mig-13* mutants is due to a loss of *unc-71* function.

To further confirm the functional link between *unc-71* and *mig-13*, we examined the effect of *unc-71* mutation on *lin-39* mutants, which exhibit anterior migration defects of QR descendants by acting in parallel to *mig-13* [17]. If *unc-71* acts in the same pathway as *mig-13*, *unc-71* should also act in parallel to *lin-39*. Consistent with this hypothesis, the migration defect of AVM neuron in *lin-39(n1760)* mutants was not rescued by the *unc-71(ov10)* mutation (Fig. S2). Taking together, these findings suggest that UNC-71 at

least partly acts downstream of MIG-13 during anterior cell migration up to the mid-body region, and that its activity has an inhibitory effect on the anterior migration of the QR and its descendants.

### 3.4. UNC-71 is expressed in a different pattern than MIG-13 and may act non-cell autonomously

To learn whether UNC-71 is expressed in QR and its descendants, we used an *unc-71-gfp* transcriptional fusion, *juIs66*. Previous work showed that *unc-71* is expressed in several head neurons, excretory cell, excretory gland cells and sphincter muscle cells in L1 to adult animals [19]. Though we were able to confirm *unc-71* expression in these cells, no significant expression was detected in the QR lineage at any stage (Fig. S3A). This suggests that UNC-71 is likely to act non-cell autonomously. We also confirmed the *mig-13* expression pattern using a *mig-13-gfp* translational fusion and the *juIs66* transgenic animal which expresses a *mig-13-mKO* transcriptional fusion. However, we could not detect co-localization of UNC-71 and MIG-13 in any cell lineages (Fig. S3B–F). These observations suggest that UNC-71 acts non-cell autonomously in cells different from MIG-13-expressing cells.

### 3.5. src-1 acts in the same pathway as mig-13 and unc-71

To further examine the potential contribution of other components to the MIG-13 pathway, we focused on the *src-1* gene. We have previously shown that SRC-1 controls the direction of cell and growth cone migration of cells including the Q neuroblasts [26]. Notably, we showed that *src-1* mutants exhibited almost the same AVM neuron distribution as *mig-13* mutants. Thus, we examined the genetic interaction of *src-1* with *mig-13* and *unc-71*. We found that the migration defect in *src-1* mutants was partially rescued in the *unc-71(ov10)* background (Fig. 3). Furthermore, *src-1(cj293); mig-13(mu225)* double mutants showed a distribution of the AVM neuron similar to that in *src-1(cj293)* mutants.

We then tested whether *src-1* is required for cells to respond to MIG-13 by expressing a *mig-13-gfp* translational fusion in *src-1(cj293)* mutants using the pan-neural H20 promoter. The *mig-13* expression promoted anterior migration of AVM neurons in wild-type, *mig-13* and *lin-39* animals; however it had no effect on *src-1(cj293)* animals (Fig. 4). These results suggest that UNC-71 acts in the same pathway as SRC-1, and that SRC-1 is tightly associated with the MIG-13 pathway.

## 4. Discussion

To address the mechanisms underlying anterior cell migration along the A/P axis, we screened for suppressors of *mig-13* mutants and identified an *unc-71/adm-1* mutation. The *unc-71* mutation suppressed the migration defect in *mig-13* mutants, allowing QR descendants to migrate anteriorly without MIG-13 activity. Expression of an *unc-71* transgene in *unc-71; mig-13* double mutants inhibited this anterior migration. These observations suggest that an unknown factor promotes anterior migration independently of MIG-13, and the activity of this factor may be suppressed by UNC-71. The fact that *unc-71* single mutants (*ju156* and *e541*) exhibit no QR anterior migration defects further indicates that UNC-71 function is suppressed in the presence of MIG-13. Taken together, these findings suggest that MIG-13 promotes the anterior migration of the QR descendants by downregulating UNC-71 function (Fig. S4).

We also found that *unc-71* mutation rescued the migration defect in *mig-13* mutants only up to the region around the V2.a cell. Also, the migration defects of the BDUR neuron in the anterior

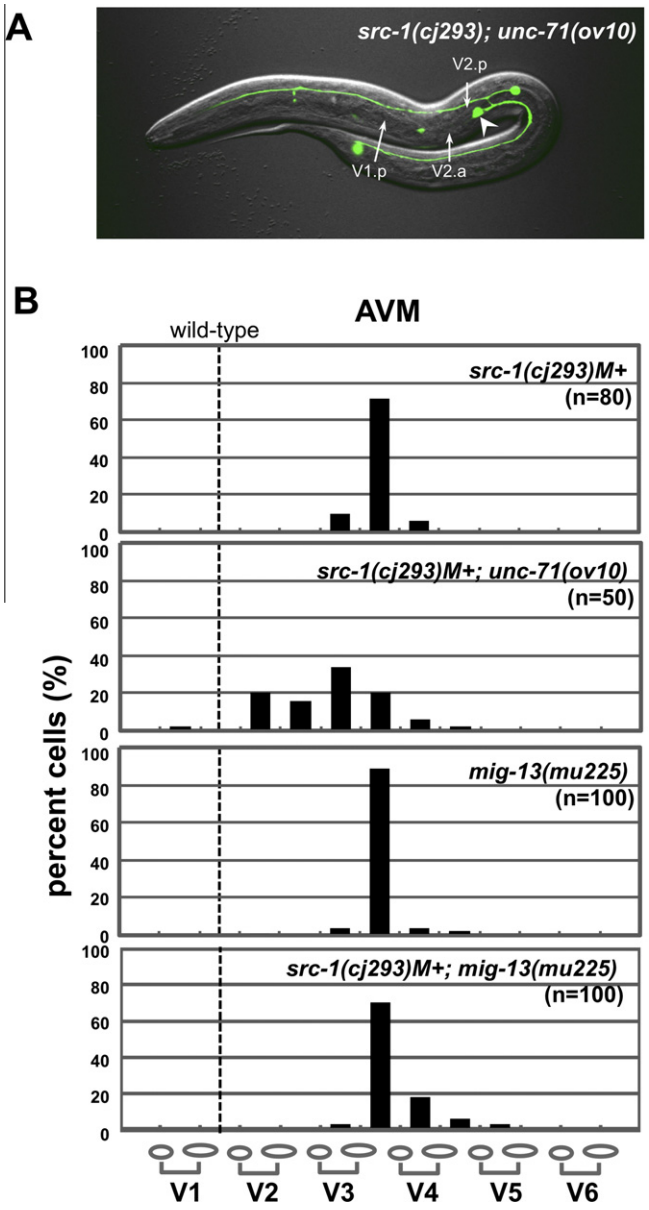


**Fig. 3.** The *unc-71* mutation suppresses the AVM neuron position defect in *src-1* mutants. (A) Typical AVM neuron position in *src-1(cj293)*; *unc-71(ov10)* mutants. AVM and other mechanosensory neurons were visualized by a *mec-7-gfp* fusion. GFP and DIC images were merged. Arrows indicate the nuclei of V-cells. The arrowhead indicates the AVM neuron. (B) Final AVM neuron positions in the indicated strains are scored. *src-1* mutants showed an AVM neuron distribution similar to that of *mig-13* mutants. In *src-1(cj293)*; *unc-71(ov10)* double mutants, the AVM neuron distribution shifted toward the anterior, and AVM neurons were located anterior to the V3.p cell. The AVM neuron distribution in *src-1*; *mig-13* double mutants was similar to that in either single mutants.

body region of *mig-13* mutants were not significantly rescued by the *unc-71* mutation. These results suggest that *unc-71* is involved in anterior migration only up to the mid-body region, and that the MIG-13 pathway may require additional factor(s) to accomplish migration to the anterior body region (Fig. S4). Thus, a more comprehensive analysis of the components of this pathway will be necessary in order to fully unravel the mechanisms of MIG-13-mediated cell migration.

UNC-71 is a member of the ADAM family of proteins, and is probably a homolog of mammalian ADAM14. Previous work has revealed that UNC-71 functions in axon guidance, axonal morphogenesis, and sex myoblast migration [19]. Since UNC-71 appears

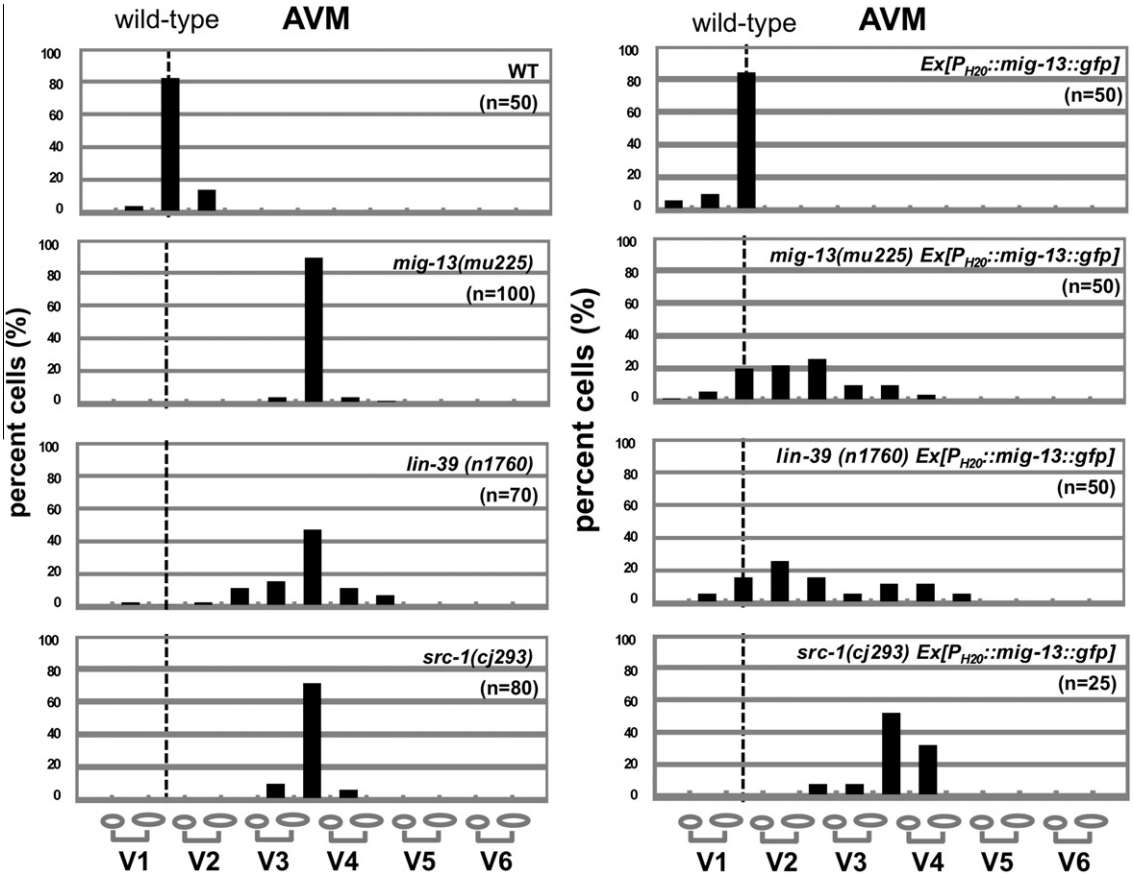


**Fig. 4.** MIG-13 requires SRC-1 to promote anterior migration. Final AVM neuron positions in the indicated strains are scored. The dashed line indicates the final position of AVM neuron in wild-type animals. Numbers scored are indicated in each graph. The AVM neuron position in *PH20::mig-13::gfp* transgenic animals (right panels) was shifted more anteriorly than its normal position except in the *src-1(cj293)* background.

not to have proteolytic activity, it may regulate target molecules via protein–protein interactions. Since mutations in the *unc-71* disintegrin and cysteine-rich domains suppress the *mig-13* mutant phenotype, it is likely that UNC-71 interacts with other components via these domains. It should also be noted that *ov10*, which likely produces an extracellular domain with an inactive metalloprotease domain, showed a stronger phenotype than that of the null *ju156*. Previous work has shown that expression of an UNC-71 mutant lacking the transmembrane domain and cytoplasmic tail induces an *unc-71* mutant-like phenotype in wild-type animals [19]. Thus, it is possible that UNC-71 must be anchored to the membrane to control the anterior migration of QR descendants, and that the inactive metalloprotease domain of the truncated UNC-71 may have another effect to enhance the *unc-71* phenotype. In this study, we showed that UNC-71 is likely to act non-cell autonomously, as reported previously [19]. These findings indicate that UNC-71 affects QR and its descendants by interacting with other targets on the surface of these cells or through some mediators. Identification of such UNC-71-related factors will be necessary to elucidate the function of UNC-71.

Recently, a novel membrane glycoprotein, LRP12/MIG13a, was identified as a mammalian homolog of MIG-13 [30]. LRP12/MIG13a is a member of the low-density lipoprotein receptor related protein (LRP) family, and regulates cell migration during neural development similarly to MIG-13. Interestingly, Reelin signaling mediated by Src family tyrosine kinases (SFKs) is required to regulate LRP12/MIG13a-positive cells. We also found that SRC-1, a *C. elegans* homolog of SFKs, is related to the MIG-13 pathway. SRC-1 controls the direction of cell and growth cone migration, including the anterior migration of the QR descendants [26,31]. However, the target molecules of SRC-1 have yet to be identified. Thus, it would be interesting to determine which components of the MIG-13 pathway can serves as substrates of SRC-1. Further mechanistic analysis of this pathway will help elucidate the molecular basis of normal cell migration in multicellular animals.

## Acknowledgments

We thank Y. Jin and C. Kenyon for kindly giving us vectors. This study was supported by the Uehara Foundation and a Grant-in-Aid for scientific research from the Ministry of Education, Culture, Sports, Science and Technology of Japan.

## Appendix A. Supplementary data

Supplementary data associated with this article can be found, in the online version, at doi:10.1016/j.febslet.2012.01.031.

## References

[1] Hedgecock, E.M., Culotti, J.G., Hall, D.H. and Stern, B.D. (1987) Genetics of cell and axon migrations in Caenorhabditis elegans. Development 100, 365–382.
[2] Antebi, A., Norris, C.R., Hedgecock, E.M. and Garriga, G. (1997). Cell and Growth Cone Migrations. In C. elegans II. Cold Spring Harbor Laboratory Press, Cold Spring Harbor, N.Y.
[3] Kurosaka, S. and Kashina, A. (2008) Cell biology of embryonic migration. Birth Defects Res. C. Embryo. Today 84, 102–122.
[4] Montell, D.J. (1999) The genetics of cell migration in Drosophila melanogaster and Caenorhabditis elegans development. Development 126, 3035–3046.
[5] Brenner, S. (1974) The genetics of Caenorhabditis elegans. Genetics 77, 71–94.
[6] Colavita, A., Krishna, S., Zheng, H., Padgett, R.W. and Culotti, J.G. (1998) Pioneer axon guidance by UNC-129, a C. elegans TGF-beta. Science 281, 706–709.

[7] Serafini, T., Kennedy, T.E., Galko, M.J., Mirzayan, C., Jessell, T.M. and Tessier-Lavigne, M. (1994) The netrins define a family of axon outgrowth-promoting proteins homologous to C. elegans UNC-6. Cell 78, 409–424.
[8] Hao, J.C. et al. (2001) C. elegans slit acts in midline, dorsal-ventral, and anterior-posterior guidance via the SAX-3/Robo receptor. Neuron 32, 25–38.
[9] Baum, P.D., Guenther, C., Frank, C.A., Pham, B.V. and Garriga, G. (1999) The Caenorhabditis elegans gene ham-2 links Hox patterning to migration of the HSN motor neuron. Genes Dev. 13, 472–483.
[10] Burdine, R.D., Chen, E.B., Kwok, S.F. and Stern, M.J. (1997) Egl-17 encodes an invertebrate fibroblast growth factor family member required specifically for sex myoblast migration in Caenorhabditis elegans. Proc. Natl. Acad. Sci. USA 94, 2433–2437.
[11] DeVore, D.L., Horvitz, H.R. and Stern, M.J. (1995) An FGF receptor signaling pathway is required for the normal cell migrations of the sex myoblasts in C. elegans hermaphrodites. Cell 83, 611–620.
[12] Sulston, J.E. and Horvitz, H.R. (1977) Post-embryonic cell lineages of the nematode, Caenorhabditis elegans. Dev. Biol. 56, 110–156.
[13] Harris, J., Honigberg, L., Robinson, N. and Kenyon, C. (1996) Neuronal cell migration in C. elegans: regulation of Hox gene expression and cell position. Development 122, 3117–3131.
[14] Kenyon, C. (1986) A gene involved in the development of the posterior body region of C. elegans. Cell 46, 477–487.
[15] Salser, S.J. and Kenyon, C. (1992) Activation of a C. elegans Antennapedia homologue in migrating cells controls their direction of migration. Nature 355, 255–258.
[16] Hunter, C.P. and Kenyon, C. (1995) Specification of anteroposterior cell fates in Caenorhabditis elegans by Drosophila Hox proteins. Nature 377, 229–232.
[17] Sym, M., Robinson, N. and Kenyon, C. (1999) MIG-13 positions migrating cells along the anteroposterior body axis of C. elegans. Cell 98, 25–36.
[18] Yang, L., Sym, M. and Kenyon, C. (2005) The roles of two C. elegans HOX co-factor orthologs in cell migration and vulva development. Development 132, 1413–1428.
[19] Huang, X., Huang, P., Robinson, M.K., Stern, M.J. and Jin, Y. (2003) UNC-71, a disintegrin and metalloprotease (ADAM) protein, regulates motor axon guidance and sex myoblast migration in C. elegans. Development 130, 3147–3161.
[20] Ch'ng, Q., Williams, L., Lie, Y.S., Sym, M., Whangbo, J. and Kenyon, C. (2003) Identification of genes that regulate a left-right asymmetric neuronal migration in Caenorhabditis elegans. Genetics 164, 1355–1367.
[21] Sulston, J.E. and Hodgkin, J. (1998) Methods The Nematode Caenorhabditis elegans, Cold Spring Harbor Laboratory, Cold Spring Harbor, N.Y..
[22] Mello, C.C., Kramer, J.M., Stinchcomb, D. and Ambros, V. (1991) Efficient gene transfer in C. elegans: extrachromosomal maintenance and integration of transforming sequences. EMBO J. 10, 3959–3970.
[23] Simmer, F., Tijsterman, M., Parrish, S., Koushika, S.P., Nonet, M.L., Fire, A., Ahringer, J. and Plasterk, R.H. (2002) Loss of the putative RNA-directed RNA polymerase RRF-3 makes C. elegans hypersensitive to RNAi. Curr. Biol. 12, 1317–1319.
[24] Schmitz, C., Kinge, P. and Hutter, H. (2007) Axon guidance genes identified in a large-scale RNAi screen using the RNAi-hypersensitive Caenorhabditis elegans strain nre-1(hd20) lin-15b(hd126). Proc. Natl. Acad. Sci. USA 104, 834–839.
[25] Fire, A., Xu, S., Montgomery, M.K., Kostas, S.A., Driver, S.E. and Mello, C.C. (1998) Potent and specific genetic interference by double-stranded RNA in Caenorhabditis elegans. Nature 391, 806–811.
[26] Itoh, B., Hirose, T., Takata, N., Nishiwaki, K., Koga, M., Ohshima, Y. and Okada, M. (2005) SRC-1, a non-receptor type of protein tyrosine kinase, controls the direction of cell and growth cone migration in C. elegans. Development 132, 5161–5172.
[27] Koch, R., van Luenen, H.G., van der Horst, M., Thijssen, K.L. and Plasterk, R.H. (2000) Single nucleotide polymorphisms in wild isolates of Caenorhabditis elegans. Genome Res. 10, 1690–1696.
[28] Wicks, S.R., Yeh, R.T., Gish, W.R., Waterston, R.H. and Plasterk, R.H. (2001) Rapid gene mapping in Caenorhabditis elegans using a high density polymorphism map. Nat. Genet. 28, 160–164.
[29] Sigurdson, D.C., Spanier, G.J. and Herman, R.K. (1984) Caenorhabditis elegans deficiency mapping. Genetics 108, 331–345.
[30] Schneider, S., Gulacsi, A. and Hatten, M.E. (2011) Lrp12/Mig13a reveals changing patterns of preplate neuronal polarity during corticogenesis that are absent in reeler mutant mice. Cereb. Cortex 21, 134–144.
[31] Hirose, T., Koga, M., Ohshima, Y. and Okada, M. (2003) Distinct roles of the Src family kinases, SRC-1 and KIN-22, that are negatively regulated by CSK-1 in C. elegans. FEBS Lett. 534, 133–138.